Supporting Information

Guest Size Limitation in Metal-Organic Framework Crystal-Glass Composites

Christopher W. Ashling,[a] Lauren K. Macreadie,[b] Thomas J. F. Southern,[a] Yiming Zhang,[b] Lauren N. McHugh,[a] Rachel C. Evans,[a] Stefan Kaskel,[c] Shane G. Telfer,[b*] and Thomas D. Bennett[a*]

[a]. Department of Materials Science and Metallurgy, University of Cambridge, Cambridge, CB3 0FS, UK.

[b]. MacDiarmid Institute for Advanced Materials and Nanotechnology, Institute of Fundamental Sciences, Massey University, Palmerston North, New Zealand.

[c]. Technische Universität Dresden, Bergstrasse 66, 01062 Dresden, Germany.

Contents:

1. Powder X-ray Diffraction
2. Thermogravimetric Analysis
3. Scanning Electron Microscopy
4. Gas Sorption

Powder X-ray Diffraction

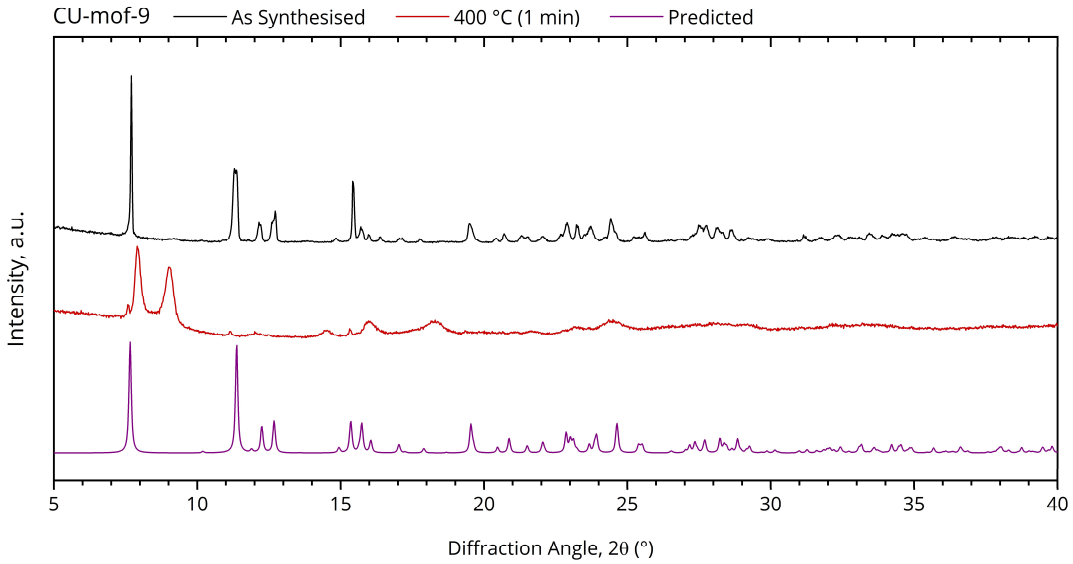

Figure S1: Powder X-ray diffraction pattern of CUmof-9 as synthesised, CUmof-9 after heating to 400 °C, and a simulated CUmof-9 PXRD pattern using published crystallographic information.[1]

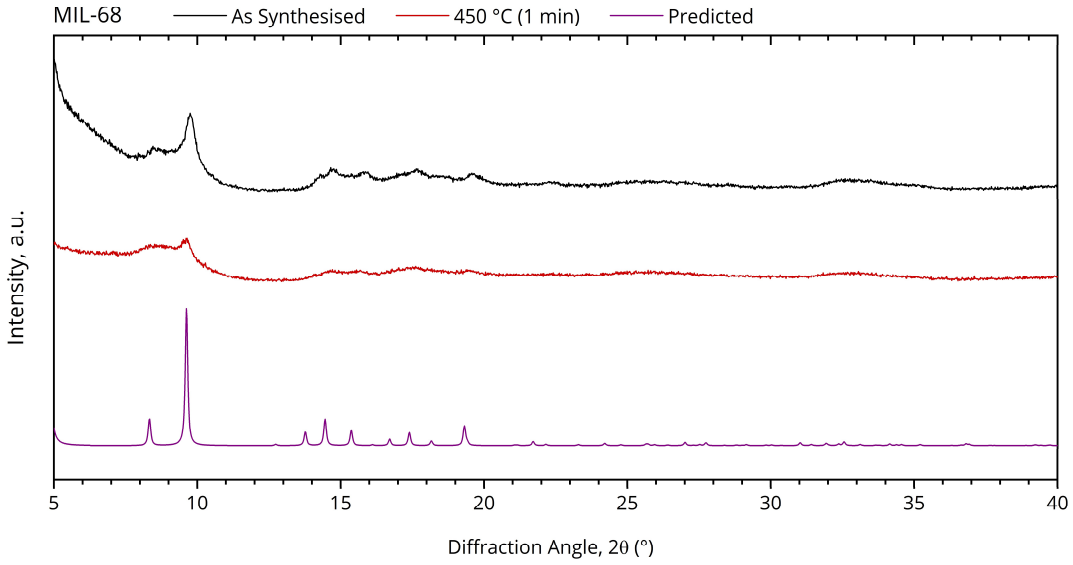

Figure S2: Powder X-ray diffraction pattern of MIL-68 as synthesised, and MIL-68 after heating to 450 °C, and simulated MIL-68 PXRD pattern using published crystallographic information.[2]

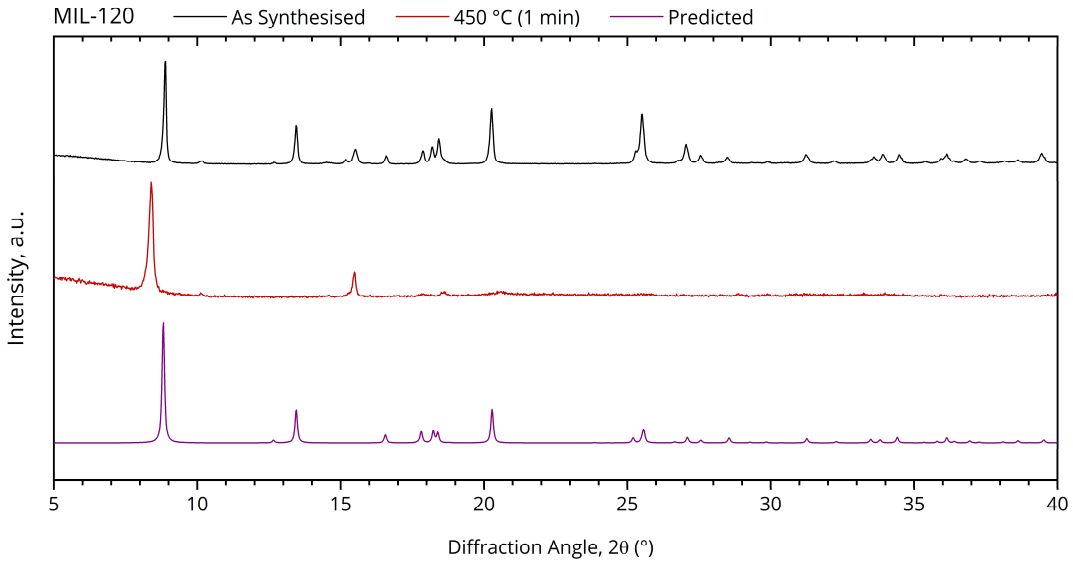

Figure S3: Powder X-ray diffraction pattern of MIL-120 as synthesised, MIL-120 after heating to 450 °C and a simulated MIL-120 PXRD pattern using published crystallographic information.[3]

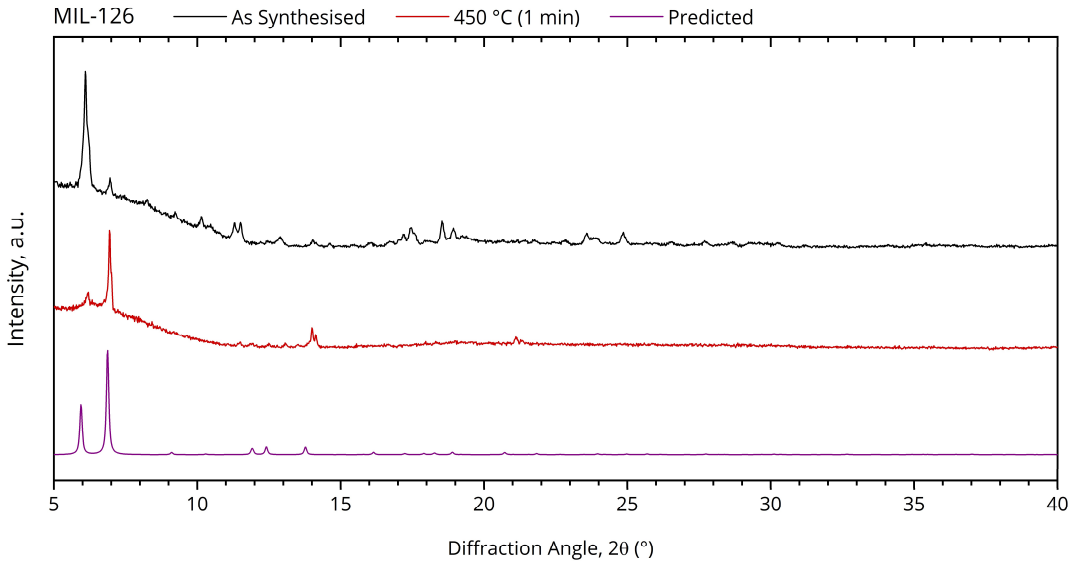

Figure S4: Powder X-ray diffraction pattern of MIL-126 as synthesised and MIL-126 after heating to 450 °C, and a simulated MIL-126 PXRD pattern using published crystallographic information.[4]

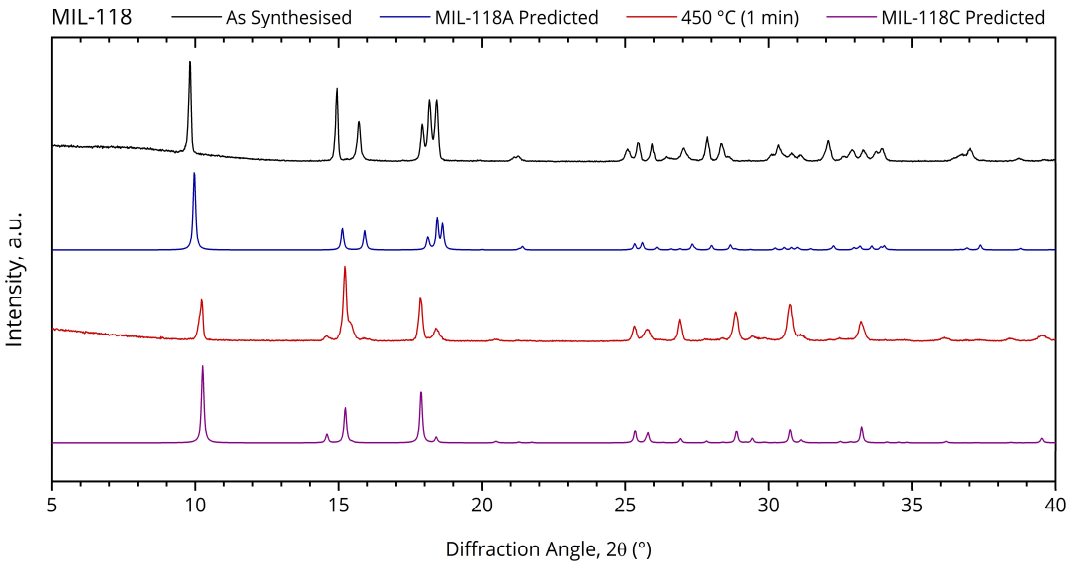

Figure S5: Powder X-ray diffraction pattern of MIL-118 as synthesised, a simulated MIL-118A PXRD pattern, MIL-118 after heating to 450 °C, and a simulated MIL-118C PXRD pattern using published crystallographic information.[5]

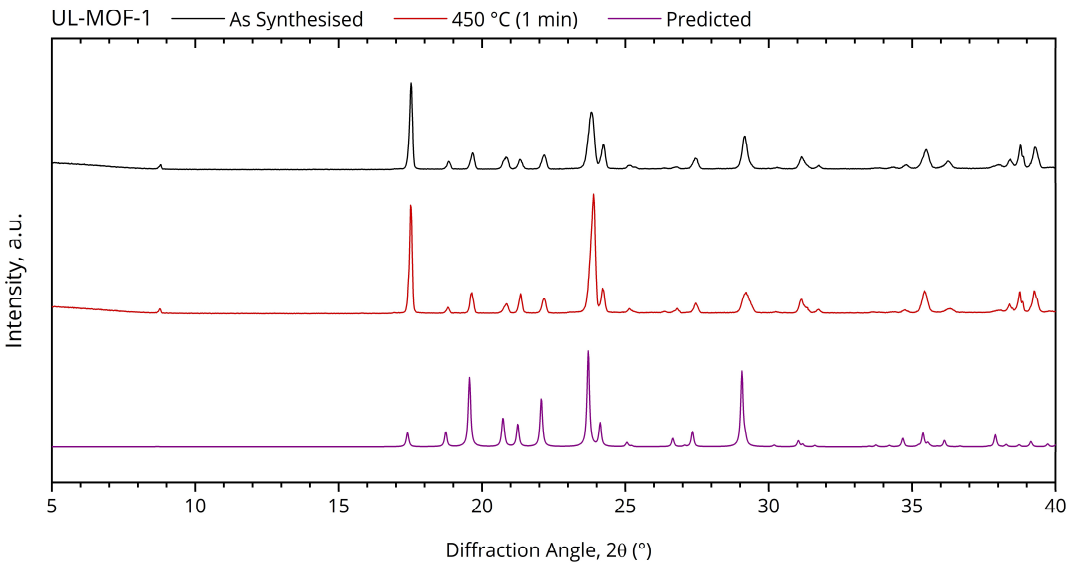

Figure S6: Powder X-ray diffraction pattern of UL-MOF-1 as synthesised and UL-MOF-1 after heating to 450 °C, and a simulated UL-MOF-1 PXRD pattern using published crystallographic information.[6]

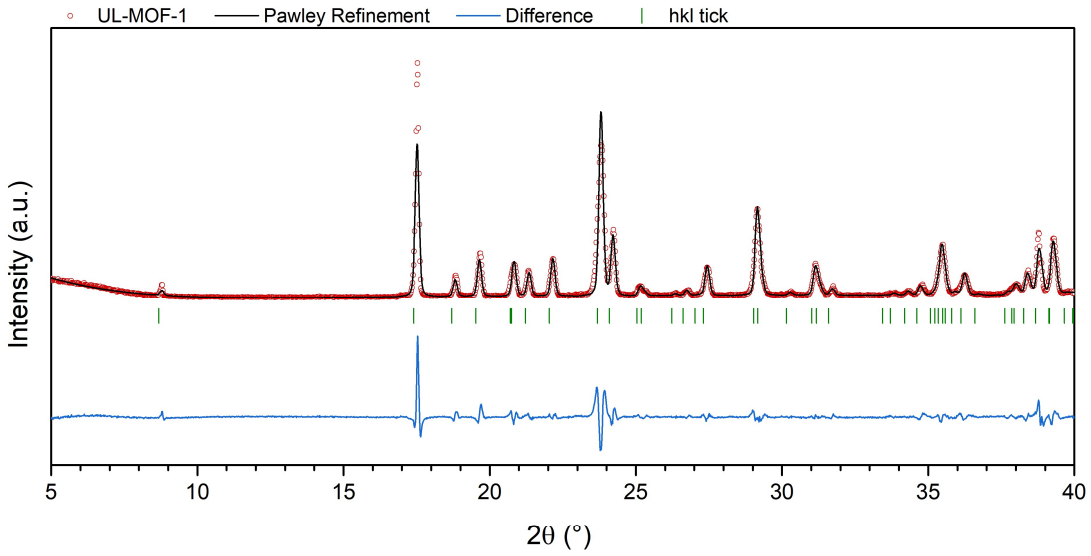

rwp: 16.064, **Space group**: P21/c, ***a***: 10.300 Å, ***b***: 5.355 Å, ***c***: 8.671 Å, ***ß***: 98.68°

Figure S7: Pawley refinement of UL-MOF-1 powder X-ray diffraction pattern.

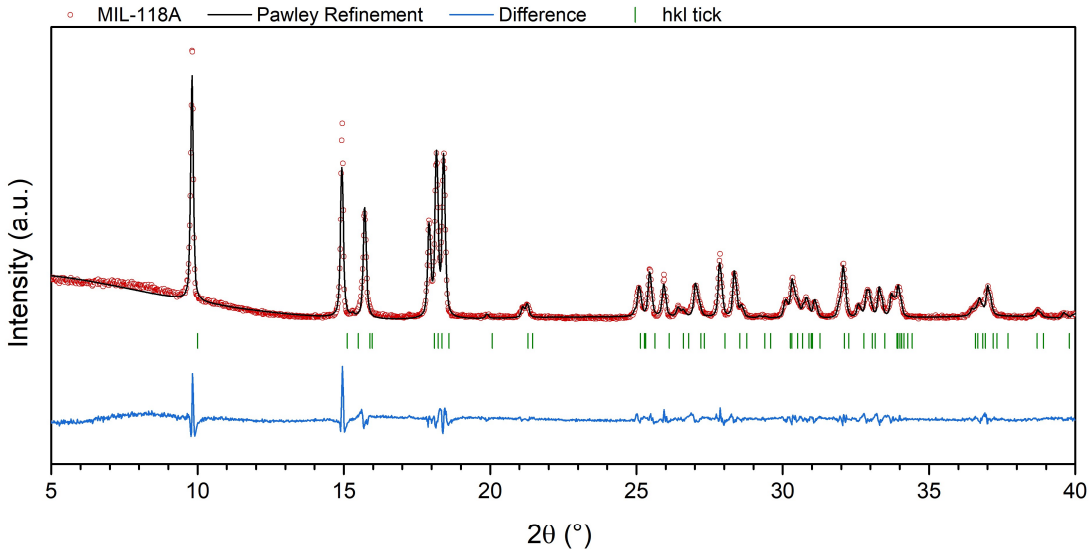

rwp: 11.945, **Space group**: C2/c, ***a***: 11.430 Å, ***b***: 6.817 Å, ***c***: 17.678 Å, ***ß***: 90.82°

Figure S8: Pawley refinement of MIL-118A powder X-ray diffraction pattern.

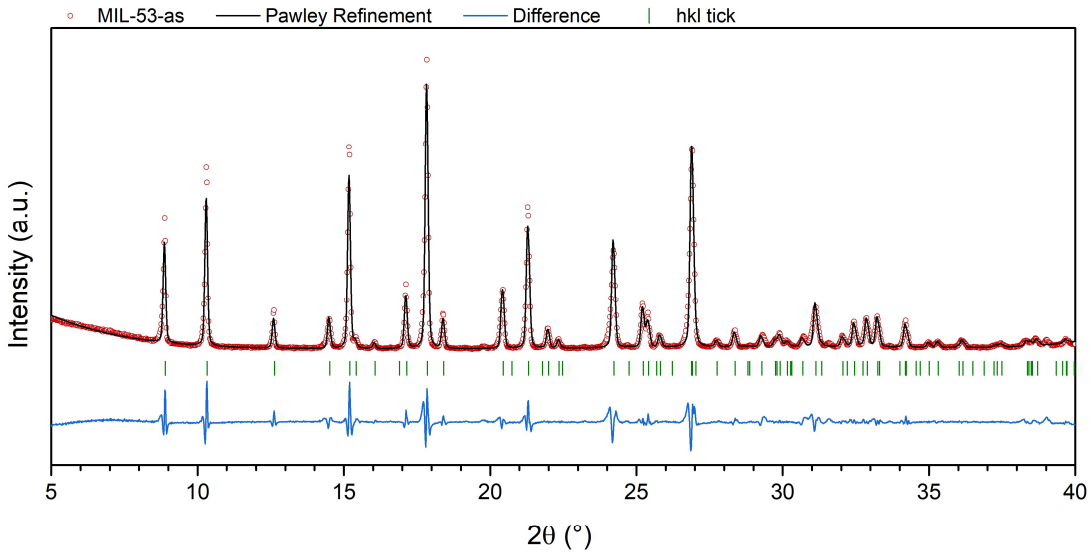

rwp: 14.291, **Space group**: Pnma, ***a***: 17.111 Å, ***b***: 6.627 Å, ***c***: 12.188 Å

Figure S9: Pawley refinement of MIL-53-as powder X-ray diffraction pattern.

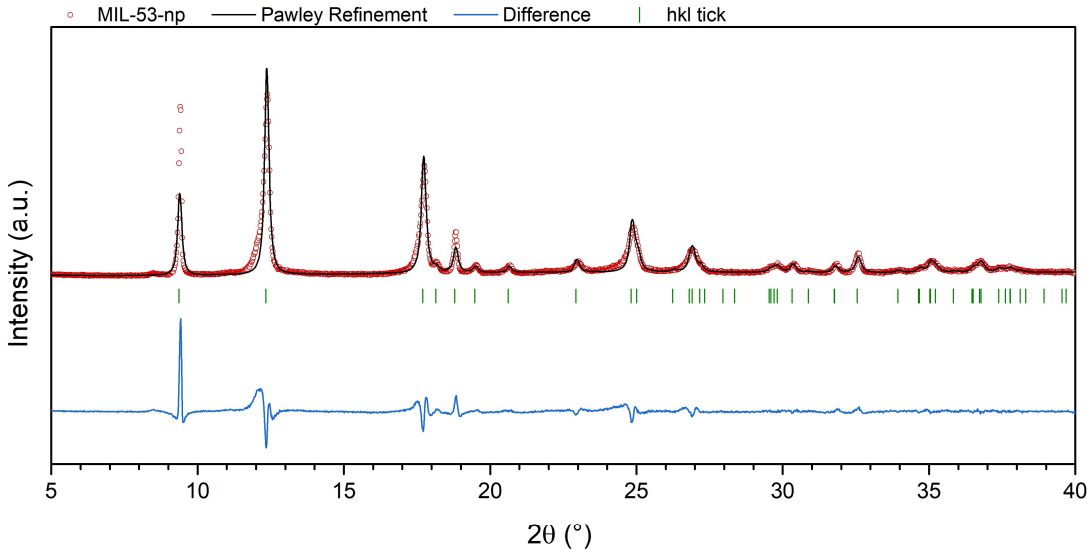

rwp: 21.783, **Space group**: Cc, ***a***: 19.494 Å, ***b***: 7.749 Å, ***c***: 6.587 Å, ***ß***: 104.54°

Figure S10: Pawley refinement of MIL-53-np powder X-ray diffraction pattern.

Table S1: Lattice parameters from published crystallographic files, and the corresponding lattice parameters of the crystalline material as determined by Pawley refinements.[3,6]

Sample	**Lattice parameters**				
	a (Å)	*b* (Å)	*c* (Å)	β (°)	Rwp
MIL-118C	12.132	6.619	17.227	90	-
$(MIL\text{-}118)_{0.5}(a_gZIF\text{-}62)_{0.5}$	12.127	6.431	17.459	90	11.152
UL-MOF-1	10.302	5.345	8.662	98.659	-
$(UL\text{-}MOF\text{-}1)_{0.5}(a_gZIF\text{-}62)_{0.5}$	10.316	5.373	8.727	98.547	7.677

Thermogravimetric Analysis

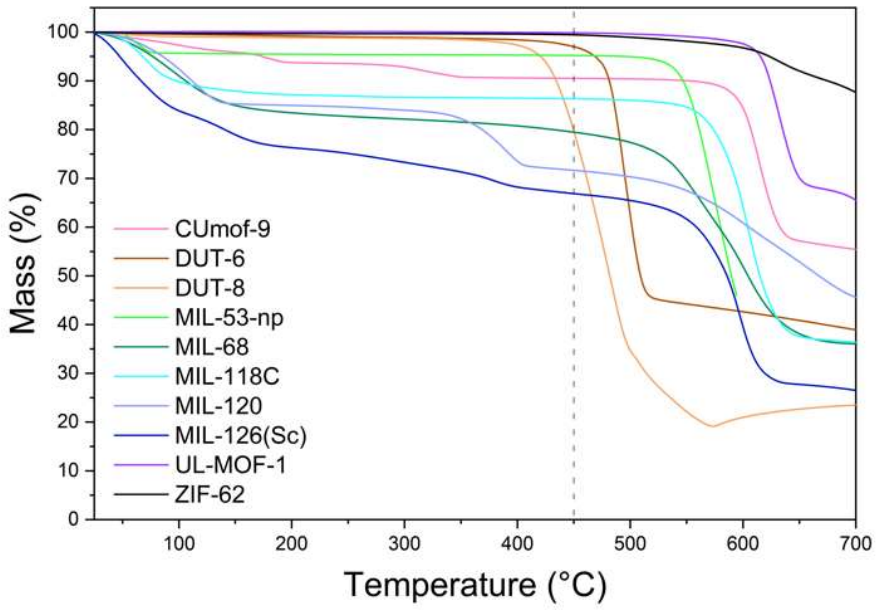

Figure S11: Thermogravimetric analysis, performed at 10 °C/min under nitrogen gas on the MOFs listed in Table 1 in the main manuscript.

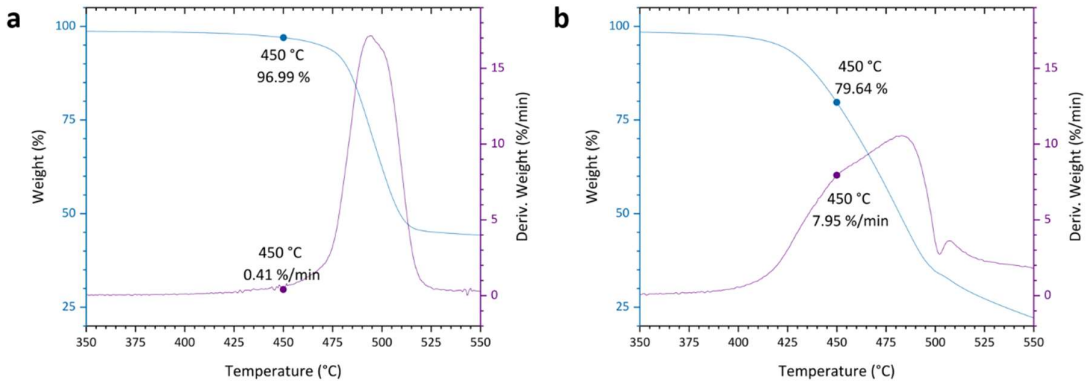

Figure S12: Thermogravimetric analysis of a) DUT-6, and b) DUT-8, displaying the normalised mass loss and the first differential of the normalised mass with respect to time. This experiment was performed at a heating rate of 10 °C/min under a nitrogen protective atmosphere.

Scanning Electron Microscopy

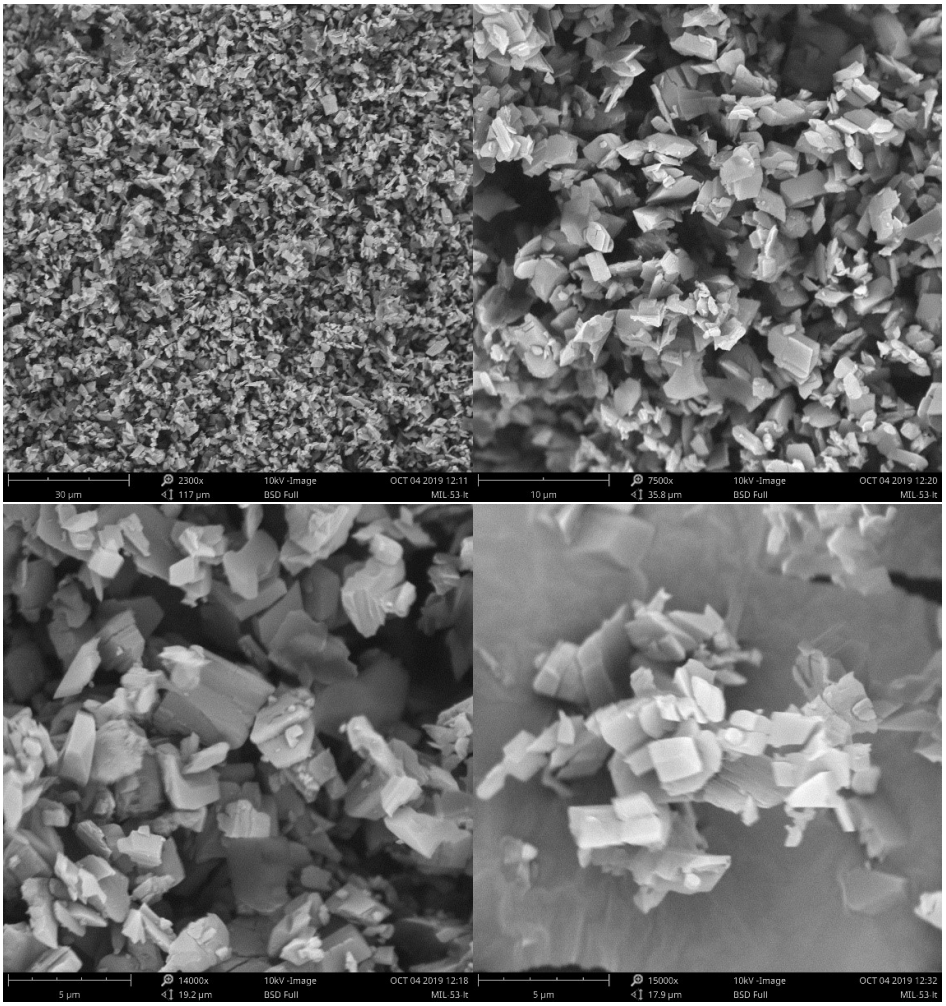

Figure S13: Scanning electron microscopy images of MIL-53-np.

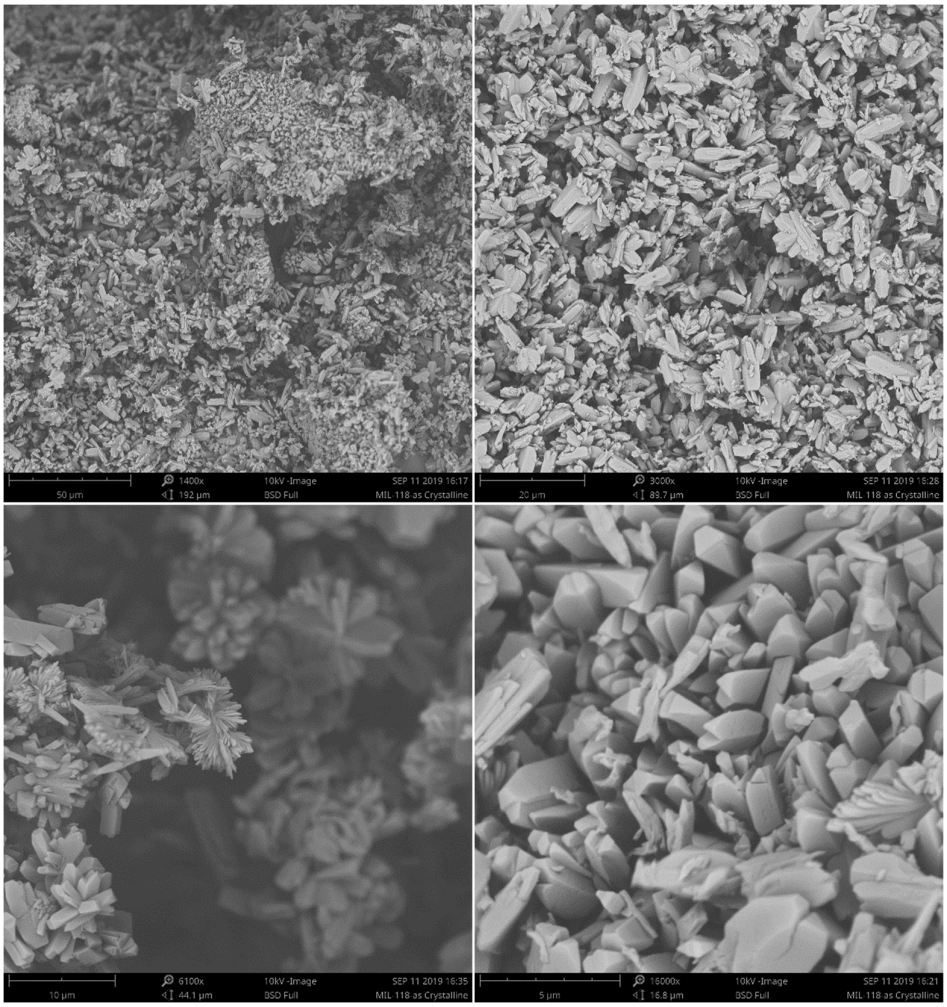

Figure S14: Scanning electron microscopy images of MIL-118C.

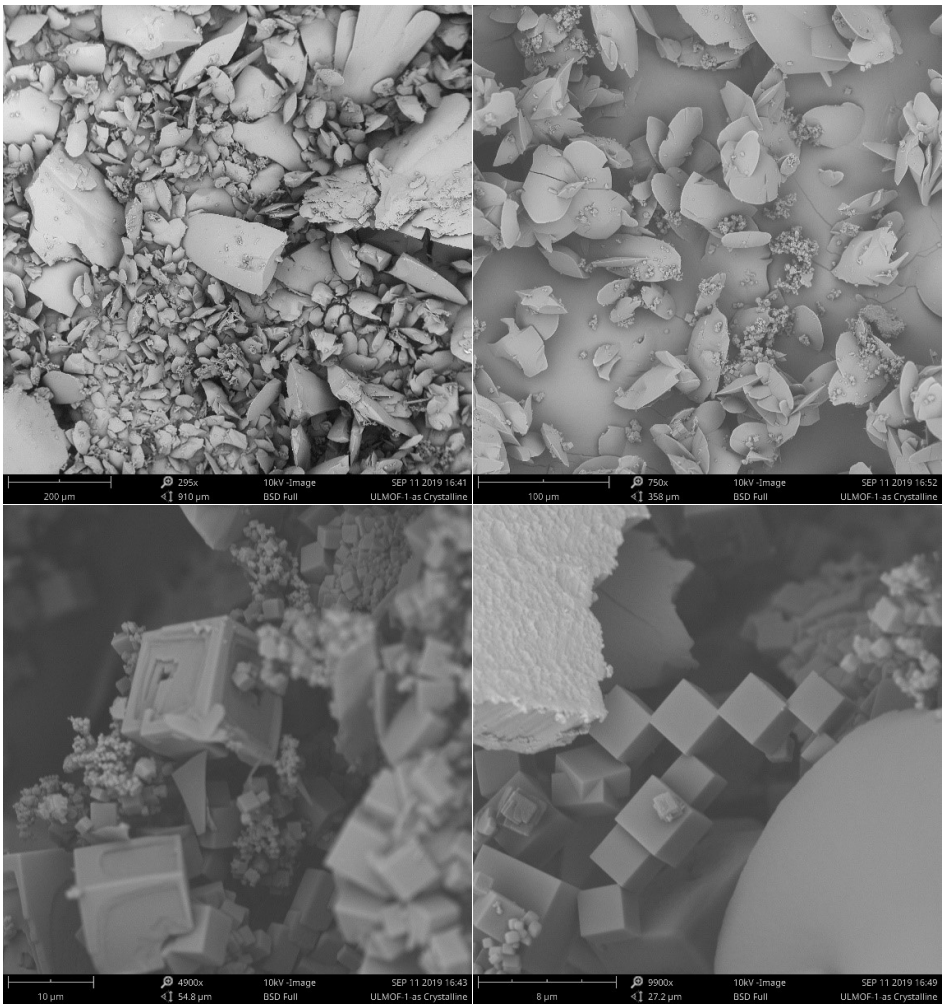

Figure S15: Scanning electron microscopy images of UL-MOF-1.

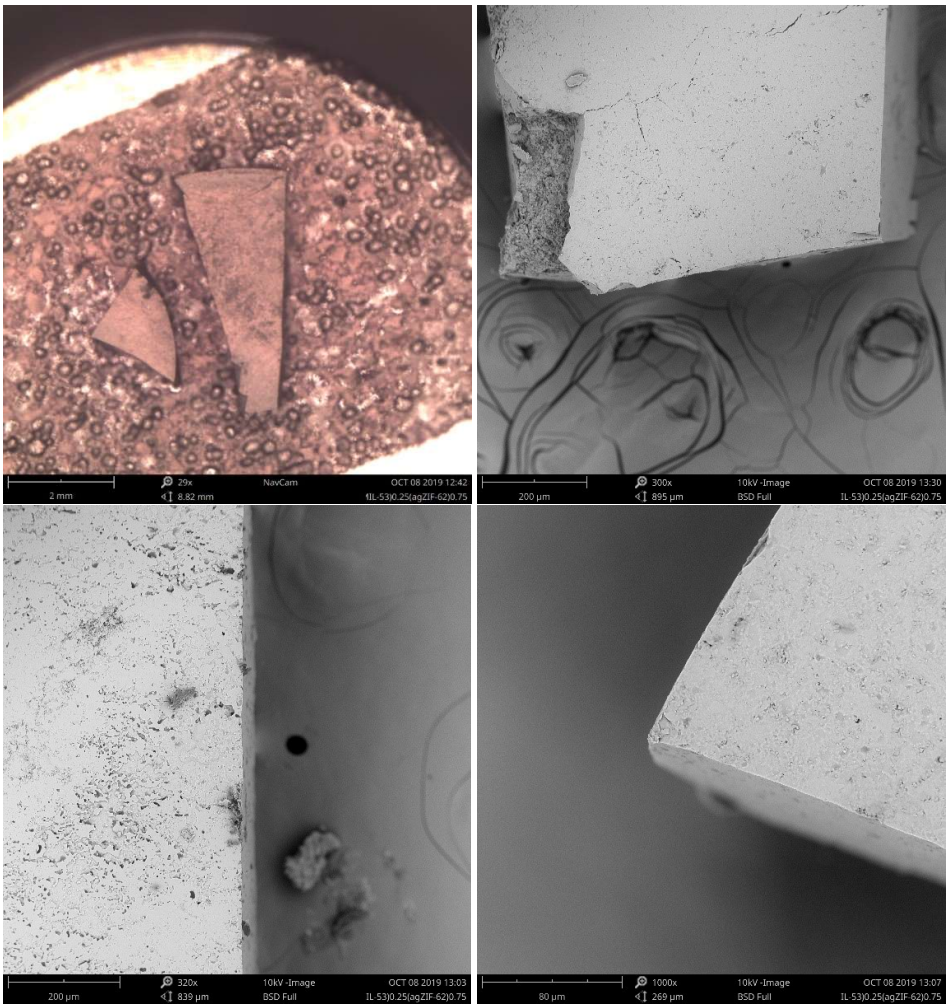

Figure S16: Optical (upper left) and scanning electron microscopy (upper right, lower left and lower right) images of a shard of $(\text{MIL-53})_{0.25}(\alpha_g\text{ZIF-62})_{0.75}$.

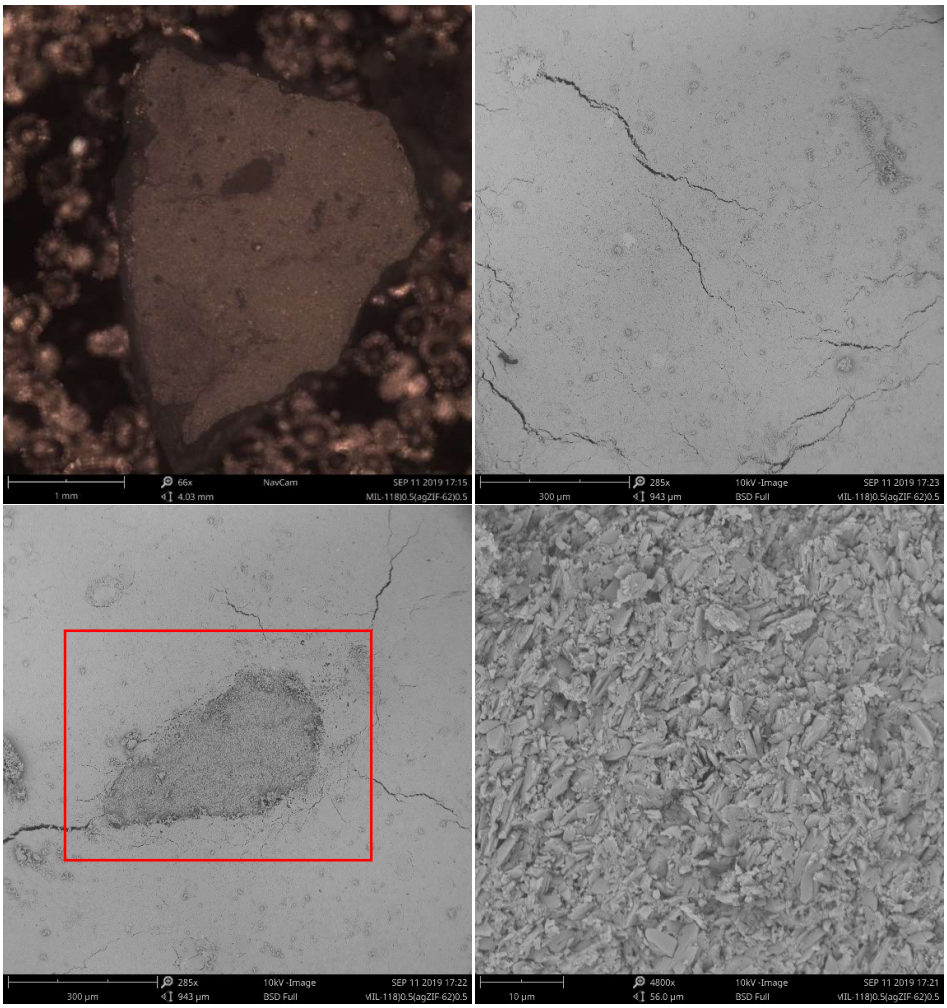

Figure S17: Optical (upper left) and scanning electron microscopy (upper right, lower left and lower right) images of a shard of $(\text{MIL-118})_{0.5}(a_g\text{ZIF-62})_{0.5}$. The lower-right image is an enhanced view of the surface defect highlighted in red.

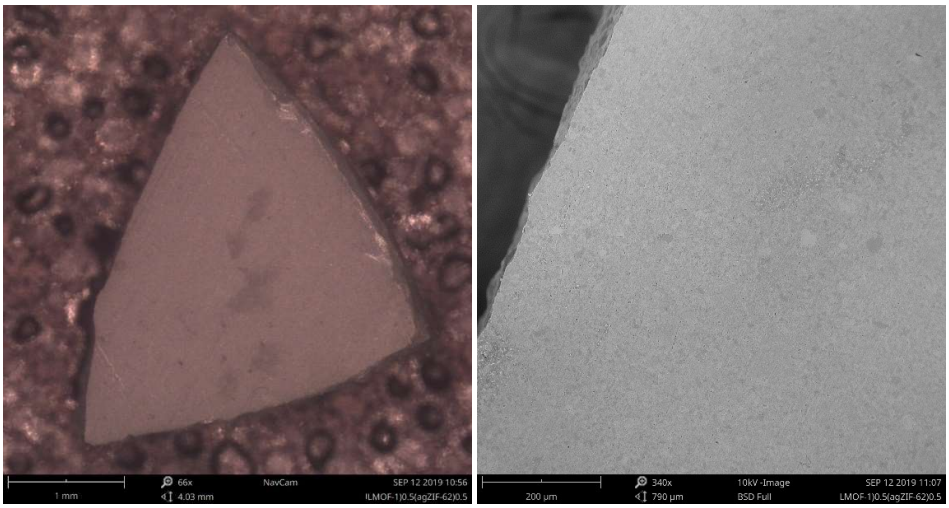

Figure S18: Optical (left) and scanning electron microscopy (right) images of a shard of (UL-MOF-1)$_{0.5}$(α_gZIF-62)$_{0.5}$.

Gas Sorption

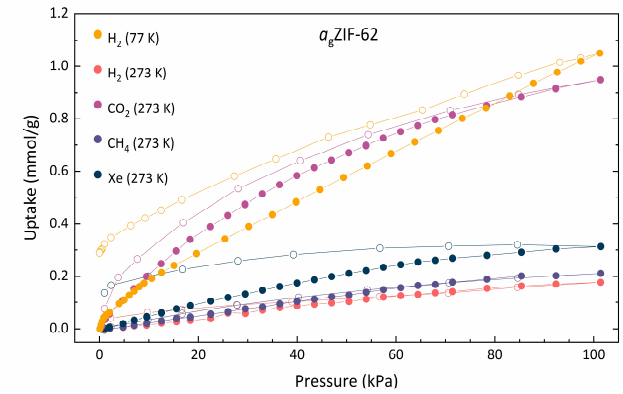

Figure S19: Gas adsorption isotherms of a_gZIF-62. Solid and open circles of the same colour indicate the adsorption and desorption respectively.

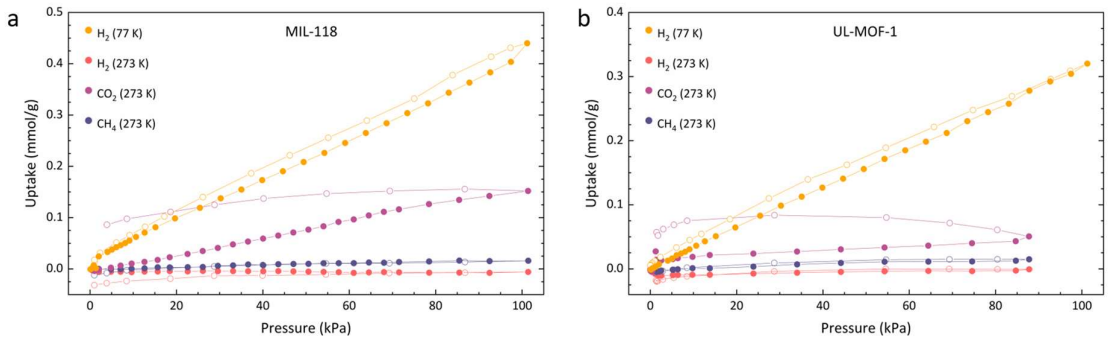

Figure S20: Gas adsorption isotherms of **a)** MIL-118, and **b)** UL-MOF-1. Solid and open circles of the same colour indicate the adsorption and desorption respectively.

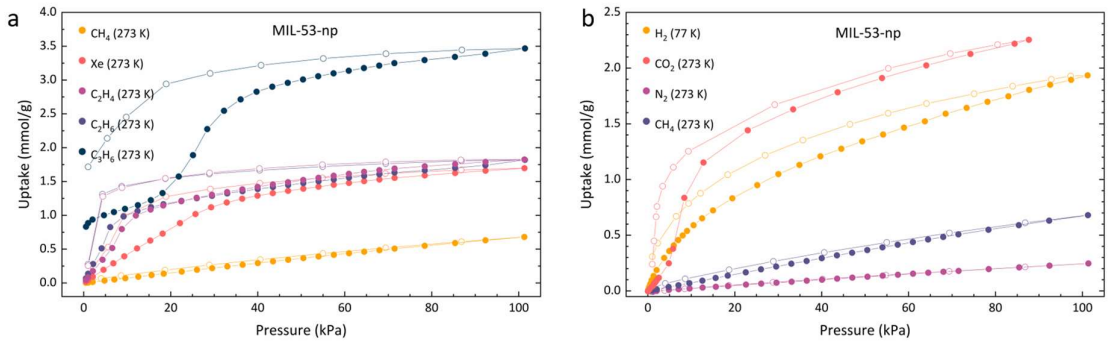

Figure S21: Gas adsorption isotherms of MIL-53-np. Solid and open circles of the same colour indicate the adsorption and desorption respectively.

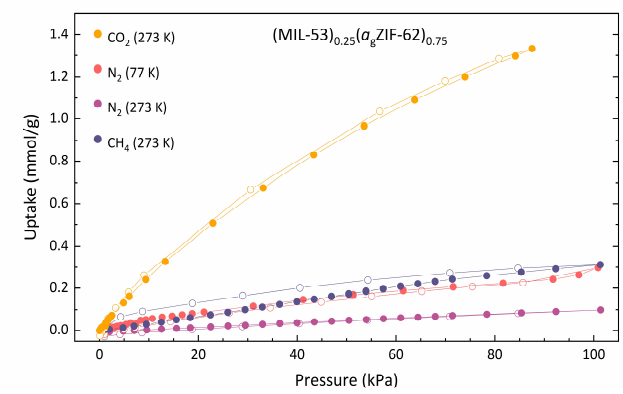

Figure S22: Gas adsorption isotherms of $(MIL\text{-}53)_{0.25}(a_gZIF\text{-}62)_{0.75}$. Solid and open circles of the same colour indicate the adsorption and desorption respectively.

References

1 F. A. A. Paz and J. Klinowski, *Chem. Commun.*, 2003, **9**, 1484–1485.

2 K. Barthelet, J. Marrot, G. Férey and D. Riou, *Chem. Commun.*, 2004, **4**, 520–521.

3 C. Volkringer, T. Loiseau, M. Haouas, F. Taulelle, D. Popov, M. Burghammer, C. Riekel, C. Zlotea, F. Cuevas, M. Latroche, D. Phanon, C. Knöfelv, P. L. Llewellyn and G. Férey, *Chem. Mater.*, 2009, **21**, 5783–5791.

4 R. J. Marshall, C. T. Lennon, A. Tao, H. M. Senn, C. Wilson, D. Fairen-Jimenez and R. S. Forgan, *J. Mater. Chem. A*, 2018, **6**, 1181–1187.

5 C. Volkringer, T. Loiseau, N. Guillou, G. Fèrey, M. Haouas, F. Taulelle, N. Audebrand, I. Margiolaki, D. Popov, M. Burghammer and C. Riekel, *Cryst. Growth Des.*, 2009, **9**, 2927–2936.

6 D. Banerjee, S. J. Kim and J. B. Parise, *Cryst. Growth Des.*, 2009, **9**, 2500–2503.